Supplementary Information

Evaluating the Potential Benefits of Metal Doped SnO_2 Negative Electrodes in Lithium Ion Batteries

Mechthild Lübke,[1,2] Ding Ning,[2] Ceilidh F. Armer,[2,3] Dougal Howard,[1] Dan J.L. Brett,[4] Zhaolin Liu[2] and Jawwad A. Darr[1]*

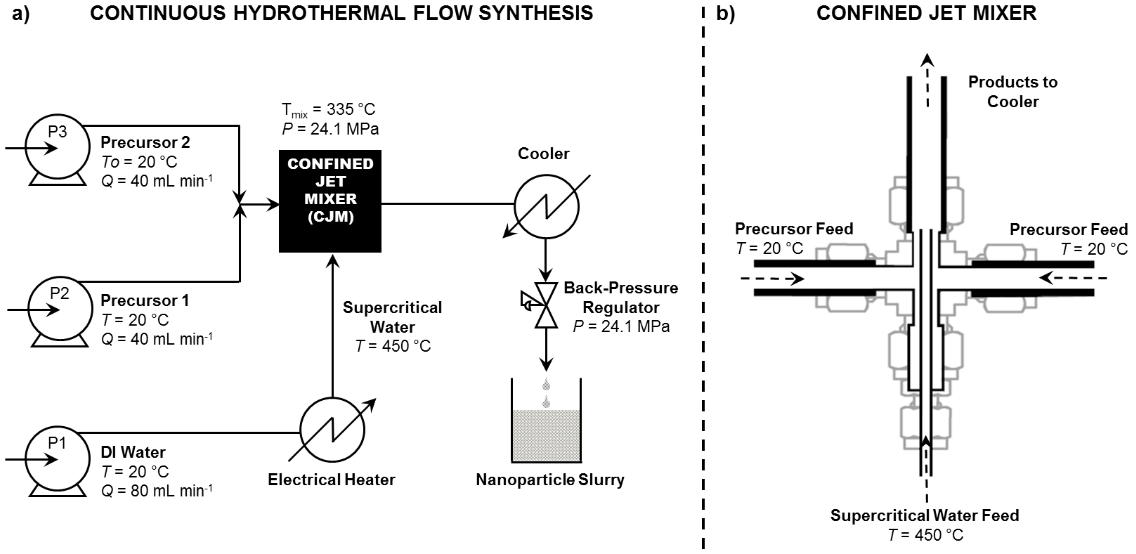

Figure S1: (a) General scheme of a CHFS pilot scale reactor (P = pump) with (b) an incorporated confined jet mixer (CJM). Pump 1 supplied a feed of DI water at a flow rate of 80 mL min^{-1}, which was then heated to 450 °C in flow using a 7 kW electrical water heater. Pump 2 supplied the Sn salt (for doped, the Sn salt was mixed with the transition metal salt in DI water) precursors at a flow rate of 40 mL min^{-1} and pump 3 supplied DI water at a flow rate of 40 mL min^{-1}. The feeds from pumps 2 and 3 were combined at room temperature in a dead volume tee-piece before this mixture was then brought into contact with the flow of supercritical water (co-currently) in the CJM to give a mixing temperature of *ca.* 335 °C (residence time *ca.* 5 s). Upon mixing of the hot and ambient temperature feeds in flow, the metal salts rapidly reacted to give the corresponding metal oxide nanoparticles that were then cooled to *ca.* 40 °C in flow via a heat exchanger. At the end of the CHFS process, each of the cooled particle-laden aqueous flows passed through a back-pressure regulator (BPR) and was collected in a beaker.

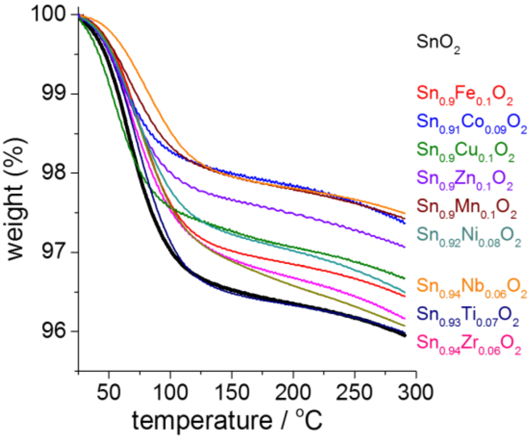

Figure S2: TGA measurements for all samples in the temperature range 25 to 300 °C.

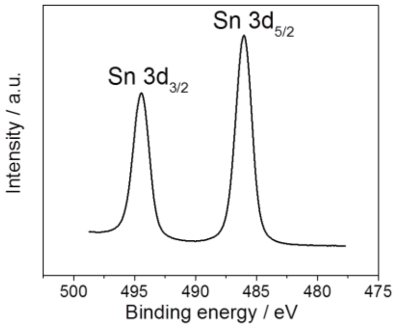

Figure S3: High-resolution XPS spectra of the Sn 3d region for undoped SnO_2.

The XPS spectra for all dopants are presented in supplementary Figure S4. For sample $Sn_{0.9}Fe_{0.1}O_2$, the Fe 2p3/2 peak could be best fitted with two components with a minor one at 710.7 eV and a major one at 715.3 eV, which were ascribed to Fe^{2+} and Fe^{3+}, respectively (Figure S2a). For sample $Sn_{0.91}Co_{0.09}O_2$, the spin-orbit splitting was 15.9 eV for the Co 2p3/2 peak at 781.1 eV and Co 2p1/2 peak at 797.0 eV, which is indicative of Co^{2+} as the main oxidation state [1] (Figure S2b). For sample $Sn_{0.9}Cu_{0.1}O_2$, there were two peaks detected corresponding to Cu 2p3/2 at 933.3 eV and Cu 2p1/2 at 953.1 eV, with spin-orbit splitting of 19.8 eV, indicative of Cu^{2+} (Figure S2c). For sample $Sn_{0.9}Zn_{0.1}O_2$, two split peaks were measured at 1021.6 eV and 1044.7 eV with a spin-orbit splitting of 23.1 eV indicative of Zn^{2+} (Figure S2d). For sample $Sn_{0.9}Mn_{0.1}O_2$, the Mn 3s region could not be investigated due to an overlap with the Sn 4p peaks. There were two peaks at 641.4 eV (major) and 644.9 eV (minor) for the Mn 3p3/2, which shows that Mn^{2+} was mainly present with some Mn^{3+} (Figure S2e). For sample $Sn_{0.92}Ni_{0.08}O_2$, the peaks at 855.8 and 873.3 eV represent the Ni^{2+} state (2p3/2 and 2p1/2, respectively), Figure S2f. The Ti 2p binding energies were 463.4 eV (Ti 2p1/2) and 457.7 eV (Ti 2p3/2), with a spin-orbit splitting of 5.7 eV; these peaks were assigned to the core levels of Ti^{4+} (Figure S2g). For sample $Sn_{0.94}Nb_{0.06}O_2$, the Nb-3d level binding energies were 209.3 eV (Nb 3d5/2) and 206.6 eV (Nb 3d3/2) with a spin-orbit splitting of 2.7 eV, which were due to the presence of Nb^{5+} (Figure S2h). For sample $Sn_{0.94}Zr_{0.06}O_2$, there were two peaks with binding energies of 182.0 and 184.4 eV that correspond to Zr 3d3/2 and Zr 3d5/2, respectively, and were representative of Zr^{4+} (Figure S2i). Thus, the oxidation state of the metal ions in the precursors did not change after the synthesis.

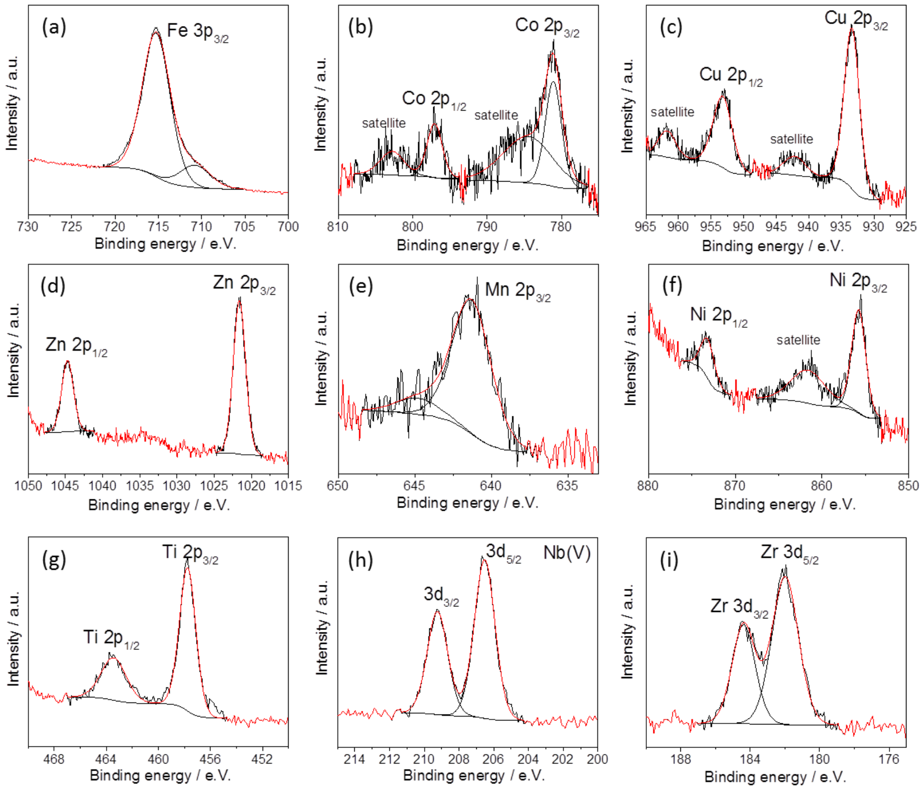

Figure S4: High-resolution XPS spectra of the splitting energies for (a) Fe 3p3/2, (b) Co 2p, (c) Cu 2p, (d) Zn 2p, (e) Mn 2p3/2, (f) Ni 2p, (g) Ti 2p, (h) Nb 3d and (i) Zr 3d orbitals.

References

[1] T.J. Chuang, C.R. Brundle, D.W. Rice, Surface Science, 59 (1976) 413-429.